Highly enhanced NO$_2$ sensing performances of Cu-doped In$_2$O$_3$ hierarchical flowers

Xiaolong Hu[a], Liyuan Tian[a], Hongbin Sun[a], Biao Wang[b], Yuan Gao[a,*], Peng Sun[a], Fengmin Liu[a], Geyu Lu[a,*]

[a] State Key Laboratory on Integrated Optoelectronics, College of Electronic Science and Engineering, Jilin University, Changchun 130012, People's Republic of China
[b] China State Key Laboratory of Luminescence and Application, Changchun Institute of Optics, Fine Mechanics and Physics, Chinese Academy of Science, Changchun 130033, People's Republic of China

ARTICLE INFO

ABSTRACT

Pure and Cu-doped hierarchical flower-like In$_2$O$_3$ microspheres constructed from numerous nanosheets have been successfully synthesized via a facile and efficient solvothermal route combined with the subsequent thermal treatment. Various techniques, including X-ray powder diffraction (XRD), field emission scanning electron microscopy (FESEM), transmission electron microscopy (TEM), and high-resolution transmission electron microscopy (HRTEM) were employed to acquire the crystalline and morphological information of the as-obtained samples. XRD measurement results apparently revealed that the lattice constants of doped products were slightly smaller than that of the pure products owing to Cu incorporation. Gas sensing performances of the sensor devices fabricated from undoped and Cu-doped In$_2$O$_3$ were systematically investigated. It was demonstrated that the Cu-doping significantly improved the response to NO$_2$. For example, sensors based on Cu-doped In$_2$O$_3$ (1.0 mol%) give a response of about 1800–400 ppb NO$_2$, which was about 14.5 times higher than sensors based on primary In$_2$O$_3$ microstructures. The excellent and enhanced NO$_2$ sensing performances of Cu-doped In$_2$O$_3$ were associated to its novel hierarchical structure and the incorporation of Cu ions.

© 2015 Elsevier B.V. All rights reserved.

1. Introduction

Nitrogen dioxide (NO$_2$), mainly produced in thermal power plant, pulp mill and vehicle, has become one of the major causes of photochemical smog, acid rain, ground-level ozone, all of which are quite harmful to our living environment. Besides, NO$_2$ is corrosive and physiological irritating, long-term inhalation would cause lung disease and RTI (respiratory tract infection), which have hazardous effect on our health. Consequently, it has become extremely significant and meaningful for the effective detection of NO$_2$. Due to the fascinating characteristics of easy manufacture, low power consumption and low cost, as well as wide detection range [1–5], gas sensor stands out from numerous detection techniques and has become a dominant approach to detect harmful gases [6–11]. It is widely acknowledged that the basic working principles of the gas sensors based on semiconductor oxides like SnO$_2$, ZnO, In$_2$O$_3$, WO$_3$ and α-Fe$_2$O$_3$ is the conspicuous resistance change which caused by reactions between the tested gases and sensing materials via the adsorption and desorption process. Hence, the composition, crystal size, surface morphology, and microstructures of oxide semiconductors play crucial roles in determining their sensing performances [5,12]. Recently, three-dimensional (3D) hierarchical microstructures assembled by nanoscaled building blocks have been attracting more and more attention as these special architectures were supposed to not only combine the merits of primary subunits, but also will show unique behaviors different from those of the nanosized subunits [13,14]. In this regard, rational design of sensing materials with novel hierarchical architectures will be of great importance for the construction of high performance sensor devices.

Indium oxide (In$_2$O$_3$), as a well-known n-type semiconductor material with a wide band gap (direct band gap around 3.6 eV), has been widely investigated in the vast array of useful applications [15–19]. Up to now, numerous literatures have reported that In$_2$O$_3$ could be utilized as a promising candidate for the effective detection of NO$_2$, O$_3$, C$_2$H$_5$OH, and so on [20–24]. Despite exciting achievements have been accomplished, the developments of higher response, lower detection limit and marked selective gas

sensors based on In_2O_3 microstructures are all still highly desirable and challenging to attain. During the past decade years, a variety of strategies including transition metal ions doping, heterostructure construction and catalyst adding were employed to get sensing performances further improved. Among them, element doping has been considered to be a simple and feasible approach to enhance the sensing properties [25–28]. Hence, efficiently combination of novel architecture of sensing material and metal ions doping will be of especially advantageous for constructing high performances sensor devices.

In this paper, pure and Cu-doped hierarchical flower-like In_2O_3 microspheres assembled by a large scale of closely interconnected nanosheets as primary building blocks were synthesized via a simple one-step solvothermal method and the subsequent annealing process. Moreover, a comparative gas sensing study between the pure and Cu-doped In_2O_3 hierarchical architectures was performed to demonstrate the superior gas sensing properties of the hierarchical Cu-doped In_2O_3 flower-like microspheres. Corresponding results clearly manifested that 1.0 mol% Cu-doped In_2O_3 microspheres presented much higher response (about 14.5 times higher than that of pure In_2O_3 at the presence of 400 ppb NO_2), faster response–recovery speed and better selectivity to NO_2 at a relatively low operation temperature (60 °C). Moreover, the sensors based on 1.0 mol% Cu-doped sample show an obvious response (about 11.8) to NO_2 even the concentration was as low as 25 ppb.

2. Experimental

2.1. Preparation of materials

All of the chemical reagents involved in the experiment were analytical grade and purchased from Sinopharm Chemical Reagent Co. Ltd. and used as received without further purification, $InCl_3 \cdot 4H_2O$ and $Cu(NO_3)_2 \cdot 3H_2O$ were used as indium and copper sources, respectively. In a typical synthesis process, 0.13 g (0.45 mmol) of $InCl_3 \cdot 4H_2O$, appropriate amount of $Cu(NO_3)_2 \cdot 3H_2O$, 1.00 g of urea and 0.26 g of sodium dodecyl sulfate (SDS) were added to 40 mL mixture of ethanol and water (1:3, v/v) under vigorous stirring. After stirring for 40 min, the homogeneous and transparent solution was transferred into a Teflon-lined stainless-steel autoclave, sealed tightly, and maintained at 160 °C for 3 h. After the autoclave was cooled to room temperature naturally, the precipitates were washed with deionized water and absolute ethanol for several times using centrifuge, and then dried at 80 °C. Finally, the dried precipitates were annealed at 500 °C for 2 h under air atmosphere with a heating rate of 2 °C/min to obtain the pure and Cu-doped flower-like In_2O_3 microspheres.

2.2. Characterization

X-ray diffraction (XRD) patterns were recorded on a Rigaku TTRIII X-ray diffractometer with Cu Kα1 radiation (λ = 1.5406 Å) in the 2θ range of 20°–70°. Field emission scanning electron microscopy (FESEM) images were obtained using a JEOL JSM-7500F microscope with an acceleration voltage of 15 kV. Transmission electron microscopy (TEM), high-resolution transmission electron microscopy (HRTEM) images, as well as selected-area electron diffraction (SAED) patterns were obtained on a JEOL JEM-3010 transmission electron microscope with an acceleration voltage of 200 kV.

2.3. Fabrication and measurement of gas sensor

Gas sensors were fabricated as follows: the as-prepared products were mixed with the deionized water in order to make a paste, subsequently, the paste was coated onto the outside of an alumina tube (4 mm in length, 1.2 mm in external diameter, and 0.8 mm in internal diameter, attached with a pair of gold electrodes which were connected with a pair of Pt wires) by a small brush to form a thick film. The Ni—Cr alloy coil was inserted into the alumina tube served as a heater, allowing us to control the operating temperature of the sensor by adjusting the heating current and the detailed fabrication process has been described in our previous literature [7]. The measurement was processed by a static process: the sensor was placed into a chamber filled with fresh air at the beginning, then a given amount of the tested gas was injected into another closed chamber by utilizing a micro-syringe and the sensor was put into the chamber for the measurement of the sensing performances. When the response reached a constant value, the sensor was put back into the first chamber which was full of fresh air and began to recover. The response of the sensor was defined as $S = R_g/R_a$ for oxidizing gas or R_a/R_g for reducing gas. Here, R_a and R_g are the resistances of the sensor in the air and the target gas, respectively. The response and recovery times are defined as the time taken by the sensor to achieve 90% of the total resistance change in the case of adsorption and desorption, respectively.

3. Results and discussion

3.1. Structural and morphological characteristics

The morphologies and microstructures of the undoped and Cu-doped In_2O_3 were characterized by FESEM. A low-magnification FESEM image exhibited in Fig. 1a clearly revealed that the as-obtained pure In_2O_3 were composed of numerous flower-like microspheres with average size of around 3 μm. In addition, it could be apparently identified that these novel hierarchical architectures were built up from abundant irregular-shaped nanosheets with a thickness of about 70 nm and the neighboring nanosheets were loosely interconnected result in the obvious open spaces exist between them, as presented in the inset of Fig. 1a. In order to observe the internal structure clearly, FESEM images of some broken flower-like microspheres were also taken and presented in Fig.A.1a and b, supplementary materials. The detailed morphology information of the nanosheets were achieved from the enlarged FESEM image shown in Fig. 1b, which indicated that these nanosheets were constructed from large amounts of densely packed nanorods with diameters about 10 nm. The typical FESEM images of the Cu-doped In_2O_3 flowers with different doping concentration (1.0 mol% and 3.0 mol%) are shown in Fig. 1c and d. It can be found that with the increase in the Cu doping amount, the integrity and the homogeneity were destroyed gradually by comparing the morphologies before and after doping, especially for the 3.0 mol% doped products.

Transmission electron microscopy (TEM), high resolution TEM (HRTEM) observations and the corresponding selected area electron diffraction (SAED) analysis were performed to provide more-detailed insight into the morphological and crystalline information of the as-prepared products. TEM images of an individual undoped and 1.0 mol% Cu-doped In_2O_3 microsphere (shown in Fig. 2a and d, respectively) further confirmed the hierarchical flower-like microsphere structure of the obtained samples, both the size and shape are in good conformity with those of the FESEM observations. The HRTEM images depicted in Fig. 2c and f expose clear lattice fringes, and the lattice fringes spacing was observed to be 0.294 nm and 0.292 nm, respectively. Both of them are in good agreement with the (2 2 2) planes of the cubic In_2O_3 structure. The circular characteristics existed in the SAED patterns (Fig. 2b and e) clearly identified that the pure and Cu-doped samples are polycrystalline structures in nature.
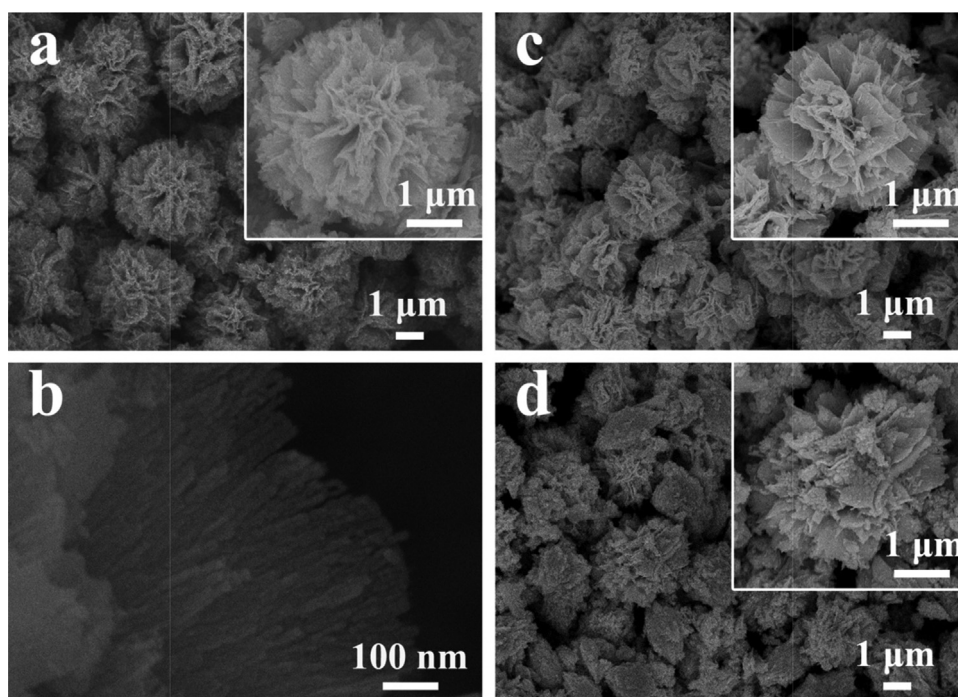
Fig. 1. A panoramic and an enlarge FESEM images of the as-synthesized In$_2$O$_3$ nanostructure with different Cu doping amount (a) 0.00 mol%, (c) 1.0 mol%, and (d) 3.0 mol%. And a high-magnification FESEM images of the as-synthesized undoped In$_2$O$_3$ structure.

X-ray powder diffraction (XRD) analysis was carried out to investigate the crystal phases of the as-synthesized samples constructed by plenty of hierarchical flower-like microstructures. And the XRD patterns are shown in Fig. 3a. In terms of the pure products, it can be seen from the XRD pattern that all the diffraction peaks could be very well indexed to the cubic structure of In$_2$O$_3$ according to JCPDS card No. 06-416, with lattice parameters of $a = 10.118$ Å. No diffraction peaks from any other impurities were observed, indicating the high purity of the products. High intensity of the diffraction peaks in the XRD pattern suggests that the sample is of high crystallinity. Likewise, with respect to the products of different Cu doping amounts, there are also no other crystalline phase or obvious peaks of impurities had been detected, implying that Cu ions would incorporate into the lattice of In$_2$O$_3$ without significantly destroying the cubic structure of indium oxide rather than generating crystalline phases of copper oxides. In order to investigate the effect of Cu doping on the phase structures of the flower-like In$_2$O$_3$ microspheres, the (2 2 2) and (4 0 0) diffraction peaks were magnified to monitor the difference between them (Fig. 3b). It was obvious that the peaks of the Cu-doped products were slightly shifted to higher 2θ values as compare with those of pure In$_2$O$_3$. The result verified that the incorporation of Cu ions led to the decreasing of lattice spacing which can be ascribed to the fact that ionic radium of Cu^{2+} (0.73 Å) is smaller than that of In^{3+} (0.80 Å). On the basis of the above XRD analysis, it can be concluded that Cu ions systematically entered the crystal lattice of flower-like In$_2$O$_3$ hierarchical structures without deteriorating the original crystal structure.

Moreover, as to further investigate the influence of the doped Cu ions, the lattice constants of pure and Cu-doped In$_2$O$_3$ were evaluated according to the Bragg's law

$$n\lambda = 2d \sin \theta \tag{1}$$

In Eq. (1), n is the order of diffraction (usually $n = 1$), λ is the X-ray wavelength, and d is the spacing between planes of given Miller

indices h, k, and l. In the cubic structure of In$_2$O$_3$, the plane spacing is related to the lattice constant a, and Miller indices by the following equation

$$\frac{1}{d_2^{(hkl)}} = \frac{h^2 + k^2 + l^2}{a^2} \tag{2}$$

So, for the (2 2 2) orientation, the lattice constant a can be calculated by

$$a = \frac{\sqrt{3}\lambda}{\sin \theta} \tag{3}$$

It can be calculated that the lattice constant a was 10.167 Å, 10.133 Å, 10.126 Å for undoped, 1 mol%, 3 mol% Cu-doped products, respectively. And the decrease in the lattice constant could be expected due to the mismatch in ionic radius.

3.2. Gas-sensing properties

In view of their peculiar structures, the as-fabricated pure and Cu-doped In$_2$O$_3$ samples were evaluated as sensing materials for chemical gas sensors. Moreover, as to demonstrate the effect of material structure on sensing properties, 1.0 mol% Cu-doped In$_2$O$_3$ nanoparticles (which were further verified by the FESEM images presented in Fig.A.2, supplementary materials) were prepared by grinding the corresponding flower-like In$_2$O$_3$ microspheres, and nanoparticles based gas sensors were also fabricated to test its sensing properties. It is well known that the gas response is greatly influenced by the operating temperature since the adsorption/desorption processes at equilibrium and the competition for chemisorptions between the tested gases and atmospheric oxygen O$_2$ for the same active surface sites are all regulated by the temperature [25]. Therefore, the responses to 400 ppb NO$_2$ for sensors based on pure, 1, 1 (NP: nanoparticles) and 3 mol% Cu-doped In$_2$O$_3$ products were tested as a function of temperature. It can be found from Fig. 4a that the responses of all these gas sensors varied
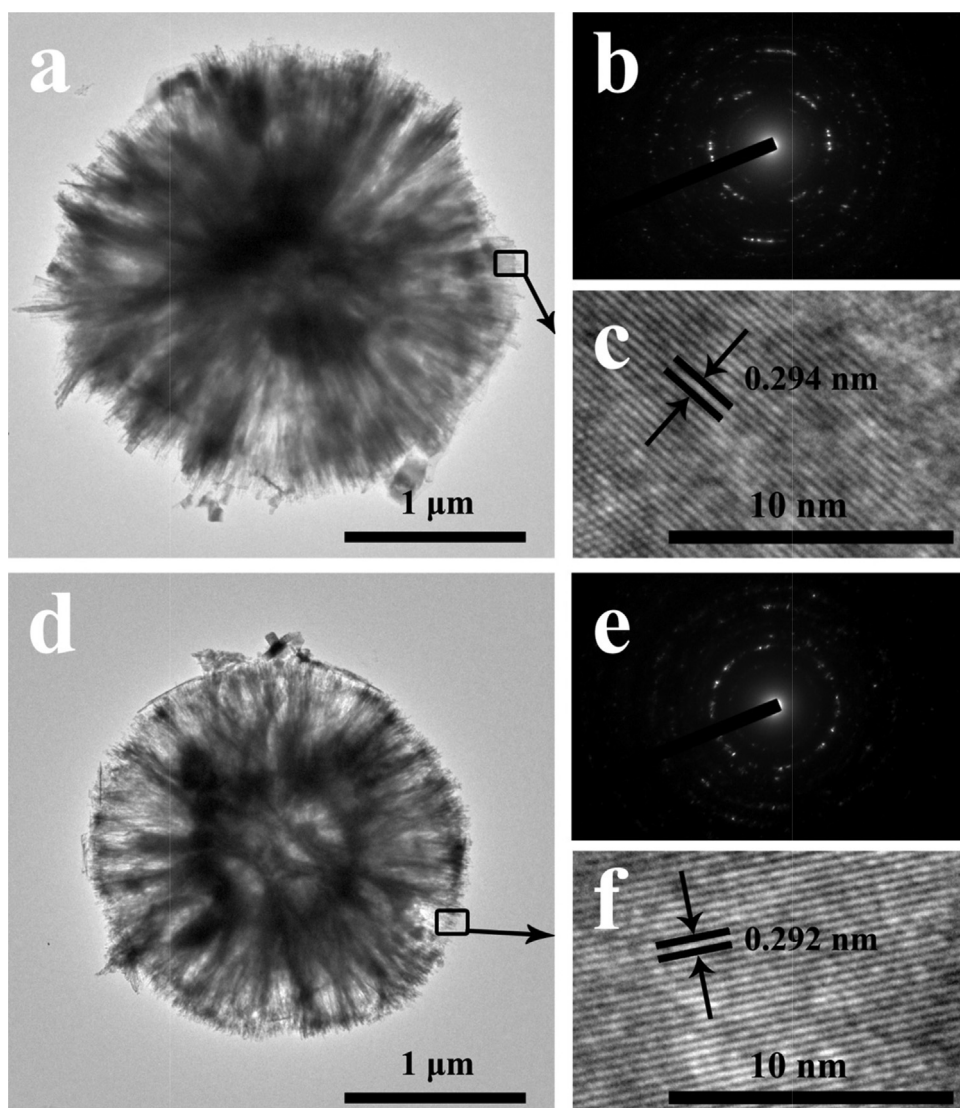
Fig. 2. (a) TEM, (b) SAED pattern and (c) HRTEM images of as-synthesized undoped In_2O_3 nanostructure. (d) TEM, (e) SAED pattern and (f) HRTEM images of as-synthesized 1.0 mol% Cu-doped In_2O_3 nanostructure.

dramatically with operating temperatures and the response values decreased with the increasing of temperature. In addition, it is obvious that gas responses of Cu-doped In_2O_3 are all improved compared with the pure one, and sensors based on the 1.0 mol% Cu-doped samples performs the best. Hence, the response time and recovery time of the sensor based on the 1.0 mol% Cu-doped sample at different temperature were calculated to determine the optimum operating temperature. The result was presented in Fig. 4b and the result showed that both the response time and recovery time decreased when the temperature increased. The activity of both the sensing material and the gas molecules would be higher as the temperature rises gives the explanatory of this trend. But meanwhile, the increase of the temperature would also lead to low diffusion depth, which was the reason why the response decreased [12]. Note that when the temperature increased from 60 °C to 80 °C, although the response decreased a lot, the response time and recovery time did not decrease that much as the temperature increased from 40 °C to 60 °C. Accordingly, the optimum temperature for these gas sensors was chosen to be 60 °C, which would be applied in all the investigations hereinafter. Besides, response transients to 400 ppb NO_2 at 60 °C of the sensors using

undoped and 1.0 mol% Cu-doped samples were measured and presented in Fig. 4c to investigate their response–recovery characteristics. It is fairly straightforward that the response time and recovery time of the sensor based on the 1.0 mol% Cu-doped sample were much shorter than that of the sensor based on the pure In_2O_3 sample. When calculated by the definitions, the response time and recovery time were about 25 min and 24 min for sensor based on pure In_2O_3 sample, while they were about 10 min and 4 min for sensor based on 1.0 mol% Cu-doped sample.

Fig. 5 reveals the relationships between sensing response and NO_2 concentration when the as-fabricated three gas sensors were exposed to NO_2 in the concentration range of 25–400 ppb at 60 °C. Apparently, all the sensors' response increased with NO_2 concentration, and Cu-doped In_2O_3 with doping amount of 1.0 mol% pales others by showing higher gas response at the same NO_2 concentration. The responses to 25, 50, 100, 200, 300, and 400 ppb NO_2 of sensors based on pure In_2O_3 sample were about 1.0, 1.2, 7.8, 25.7, 68.6, and 124.1, while the responses were 11.8, 32.4, 114.0, 259.6, 1053.9, and 1800.1 for sensors based on the 1.0 mol% Cu-doped In_2O_3 flower-like microspheres, 3.9, 9.7, 44.4, 193.7, 424.8, and 914.8 for sensors based on 1.0 mol% Cu-doped In_2O_3
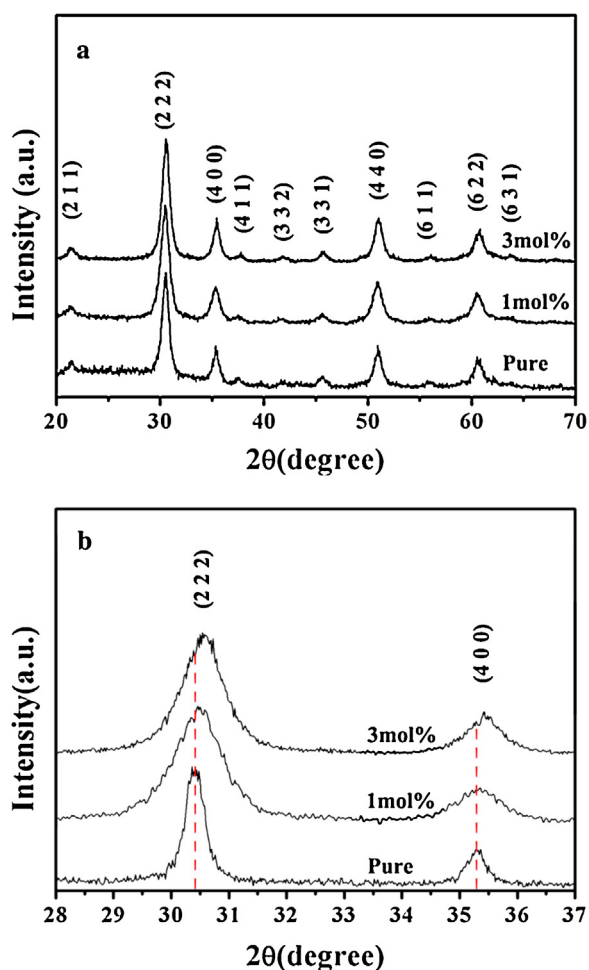
Fig. 3. (a) XRD pattern of samples with different Cu doping amount. (b) Comparison of (2 2 2) and (4 0 0) peaks from XRD patterns.

Fig. 4. (a) Response versus operation temperature of sensors based on undoped and Cu-doped In_2O_3 sample with different doping amount to 400 ppb NO_2 (NP: nanoparticles). (b) The correlation of the response/recovery times to 400 ppb NO_2 with the operation temperature for sensors based on 1.0 mol% Cu-doped In_2O_3 sample. (c) Response transient of sensors based on undoped and 1.0 mol% Cu-doped flower-like In_2O_3 microspheres to 400 ppb NO_2 at the optimum operation temperature (60 °C).

nanoparticles, and 1.4, 4.0, 20.7, 171,334.6, and 1042.6 for the sensor based on the 3.0 mol% Cu-doped In_2O_3 sample. It can be calculated that the response to 400 ppb NO_2 at 60 °C of the 1.0 mol% Cu-doped In_2O_3 sample was 14.5 times higher than that of the sensor based on pure In_2O_3 sample. Besides, it is noteworthy that the sensor based on 1.0 mol% Cu-doped In_2O_3 hierarchical flowers show an obvious response (about 11.8) to NO_2 even the concentration was as low as 25 ppb, while the response of sensor based on pure In_2O_3 to 50 ppb NO_2 was only about 1.2, which indicated that the sensor had a low detection limit. Besides, when compared the performance of sensors based on 1.0 mol% Cu-doped In_2O_3 nanoparticles with these based on the 1.0 mol% Cu-doped In_2O_3 nanoflowers, it can be found that the sensing properties has degraded by more than half. The higher responses of the nanoflowers sample are due to its hierarchical structure which can provide a larger surface-to-volume ratio and better surface permeability that can greatly facilitate the gas diffusion and mass transport in sensing material [13].

From the perspective of practical application, selectivity is another important parameter for a gas sensor. Consequently, selectivity of the gas sensors fabricated from pure and 1.0 mol% Cu-doped products were evaluated by exposing sensors to different tested gases at the optimum temperature of 60 °C. The corresponding test data were summarized and displayed in Fig. 6 in the form of bar chart. It can be seen clearly that the response values changed little for the majority of tested gases (such as HCHO, CH_3OH,
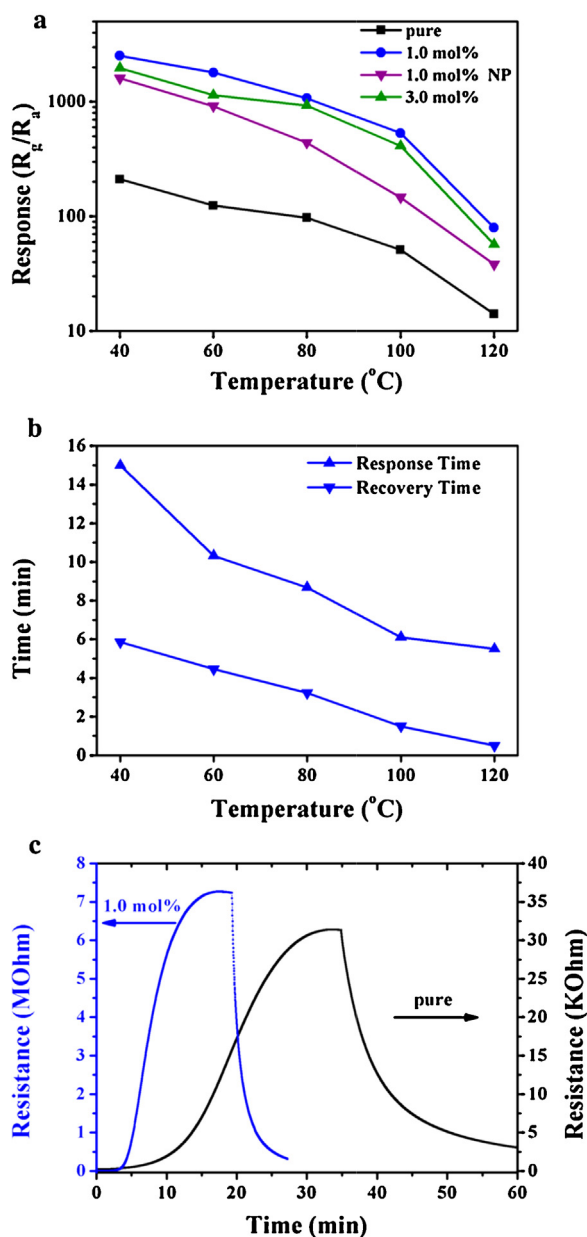
C_2H_5OH, and CO) before and after Cu doping process, while a relatively dramatic enhancement in O_3, Cl_2 and NO_2 sensing properties can be acquired. Moreover, it should be noticed that 1.0 mol% Cu-doped In_2O_3 flower-like structures exhibit much higher response to 400 ppb NO_2 than all the residual test gases, which were even tested at a higher concentration. All the measurement results unambiguously proved that the 1.0 mol% Cu-doped In_2O_3 shows superior selectivity to NO_2.

Considering that the low operation temperature (60 °C) which means low power consumption, the sensors fabricated from the 1.0 mol% Cu-doped products with features of high response, low detection limit and good selectivity shed light on new promising candidates for the practical application in atmospheric pollution monitoring.

Table 1
Comparison of gas-sensing characteristics of sensing material in present work and those reported in the literatures.

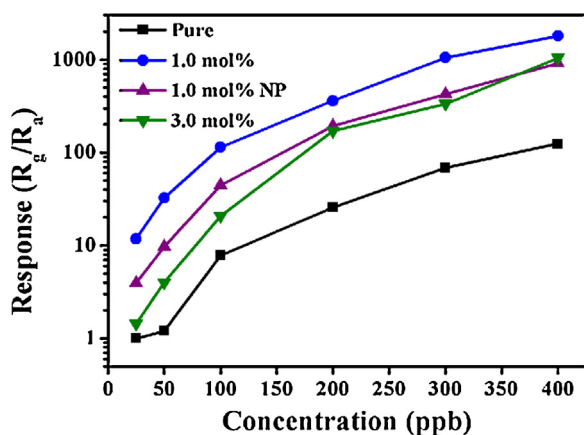| Material	NO_2 concentration	Temperature	Response	Response time	Recovery time	Reference
Ordered mesoporous Fe-doped In_2O_3	1 ppm	150 °C	71	5 min	3 min	[30]
Porous In_2O_3	50 ppm	250 °C	164	5 s	14 s	[31]
Root slice-like In_2O_3 microspheres	20 ppm	250 °C	~36	5 s	20 s	[32]
Zn-doped flower-like In_2O_3	50 ppm	300 °C	821.7	2 s	6 s	[33]
WO_3 thin films	10 ppm	150 °C	~57	14 min	8 min	[34]
DBSA doped PPy—WO_3	5 ppm	38 °C	11	6 min	18 min	[35]
In_2O_3 flower-like microspheres	400 ppb	60 °C	124.1	25 min	24 min	Present work
Cu—In_2O_3 flower-like microspheres	400 ppb	60 °C	1800	10 min	4 min	Present work

Fig. 5. Response of sensors based on undoped, 1.0 mol%, 1.0 mol% (NP: nanoparticles) and 3.0 mol% Cu-doped In_2O_3 nanostructure versus NO_2 concentrations at the optimum operation temperature (60 °C).
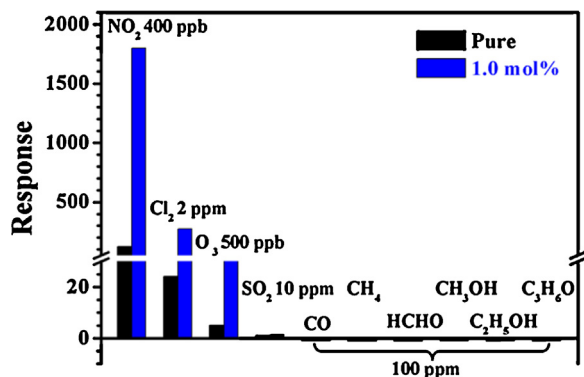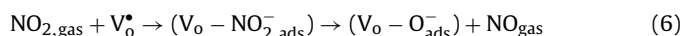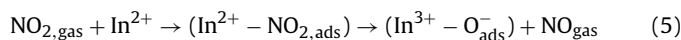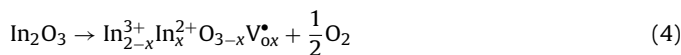

Fig. 6. Response of sensors based on undoped and 1.0 mol% Cu-doped flower-like In_2O_3 microspheres to different test gases when the operation temperature is 60 °C.

A comparison between the sensing performances of the sensor presented in this paper and literature reports is summarized in Table 1. As can be seen from the table, the sensor presented in our work exhibits better sensing performance than those reported in the literatures [29–34].

For sensors based on semiconductor oxide like In_2O_3, the most widely accept sensing mechanism when the target gas is NO_2 can be stated as follow. The electrical conductivity of In_2O_3 is attributed to electron transfer between In^{2+} and In^{3+}, the formation of the In^{2+} occurring through oxygen deficiency (Eq. (1)). Anion vacancies $V_o^\bullet$ and mainly partially reduced cations In^{2+} are the surface basic sites $(S_b)_s$ for NO_2 chemisorption. And the formation of the chemisorption bond continued on the charge transfer from active sites $(S_b)_s$ into an orbital of NO_2 causes a reduction in the strength of the N—O bonds that makes easier the decomposition of the NO_2

molecules. Therefore, NO_2 molecules were reduced into NO or N_2 molecules and the electronics of the In_2O_3 sensing materials were captured which led to the increase of the resistance of the sensor. The sensing mechanism could be summarized according to the following equations [35,36].

$$In_2O_3 \rightarrow In_{2-x}^{3+}In_x^{2+}O_{3-x}V_{ox}^\bullet + \frac{1}{2}O_2 \tag{4}$$

$$NO_{2,gas} + In^{2+} \rightarrow (In^{2+} - NO_{2,ads}) \rightarrow (In^{3+} - O_{ads}^-) + NO_{gas} \tag{5}$$

$$NO_{2,gas} + V_o^\bullet \rightarrow (V_o - NO_{2,ads}^-) \rightarrow (V_o - O_{ads}^-) + NO_{gas} \tag{6}$$

When Cu ions were doped into the flower-like In_2O_3 microspheres, some In^{3+} were substituted by Cu^{2+}, and this substitution will be compensated by the generation of either holes or indium interstitials. The generated holes will recombine with the electrons which are the major carriers of In_2O_3. And the electrons near the opposite charge of the indium vacancies will be restricted. In all these two cases, the electron concentration in the conduction band of the In_2O_3 sensing materials will be decreased which will lead to the decrease of the conductivity of the sensing materials. In the actual test, the R_a of the sensor based on the undoped, 1.0 mol% Cu-doped and 1.0 mol% Cu-doped In_2O_3 hierarchical nano structure were about 200 Ω, 4 kΩ and 150 kΩ, respectively. So the test results agree well with the theoretical analysis. When the electron concentration of the conductivity band of the sensing materials decreased, the resistance change R_g/R_a, that is, the response of the sensor will be higher when the same amount of electrons taken by the NO_2 molecules. Besides, copper oxide-supported catalysts have been reported to show activity for NO_x abatement with different reducing agents [37,38]. So it is an acceptable speculation that the cupric ions being doped into the In_2O_3 may have the function to promote the reaction described in Eqs. (2)–(4), which will lead to a higher response and shorter response time. But when the doping amount is too high, 3.0 mol%, for example, the hierarchical nanostructure will be destroyed and its sensing properties will be degraded due to the aggregation of the nanoparticles which will led to low sensing material utilization and low diffusion efficiency [12]. Therefore, sensors based on 3.0 mol% Cu-doped In_2O_3 sample did not performance as well as these based on 1.0 mol% Cu-doped In_2O_3 sample, but still much better than these based on pure In_2O_3 hierarchical flowers.

4. Conclusion

In summary, a facile and efficient solvothermal strategy combined with the following calcinations process for the synthesis of hierarchical undoped and Cu-doped In_2O_3 microstructures has been developed. FESEM and TEM observations unambiguously demonstrated that the flower-like microspheres were built from numerous nanosheets which were constructed from large quantity of nanorods. When evaluated as sensing materials for gas sensors, the as-prepared 1.0 mol% Cu-doped In_2O_3 hierarchical flowers manifest an impressive NO_2 sensing performance with

high response, excellent selectivity, and low detection limit at a low operating temperature. It is supposed that outstanding NO_2 sensing properties of the hierarchical Cu-doped In_2O_3 sample was attributed to the synergistic effects of its hierarchical nanostructure, the decreased carrier concentration and the possible catalysis action of Cu ions.

Acknowledgments

Appendix A. Supplementary data

Supplementary data associated with this article can be found, in the online version, at http://dx.doi.org/10.1016/j.snb.2015.06.080

References

[1] D.E. Williams, Semiconducting oxides as gas-sensitive resistors, Sens. Actuators B: Chem. 57 (1999) 1–16.
[2] N. Barsan, M. Schweizer-Berberich, W. Gopel, Fundamental and practical aspects in the design of nanoscaled SnO_2 gas sensors: a status report, Fresenius J. Anal. Chem. 365 (1999) 287–304.
[3] G. Korotcenkov, Gas response control through structural and chemical modification of metal oxide films: state of the art and approaches, Sens. Actuators B: Chem. 107 (2005) 209–232.
[4] G. Eranna, B.C. Joshi, D.P. Runthala, R.P. Gupta, Oxide materials for development of integrated gas sensors – a comprehensive review, Crit. Rev. Solid State Mater. Sci. 29 (2004) 111–188.
[5] N. Barsan, D. Koziej, U. Weimar, Metal oxide-based gas sensor research: how to? Sens. Actuators B: Chem. 121 (2007) 18–35.
[6] D.J. Yang, I. Kamienchick, D.Y. Youn, A. Rothschild, I.D. Kim, Ultrasensitive and highly selective gas sensors based on electrospun SnO_2 nanofibers modified by Pd loading, Adv. Funct. Mater. 20 (2010) 4258–4264.
[7] X.W. Li, P. Sun, T.L. Yang, J. Zhao, Z.Y. Wang, W.N. Wang, Y.P. Liu, G.Y. Lu, Template-free microwave-assisted synthesis of ZnO hollow microspheres and their application in gas sensing, CrystEngComm 15 (2013) 2949–2955.
[8] F. Zhang, A.W. Zhu, Y.P. Luo, Y. Tian, J.H. Yang, Y. Qin, CuO nanosheets for sensitive and selective determination of H_2S with high recovery ability, J. Phys. Chem. C 114 (2010) 19214–19219.
[9] J.Y. Liu, T. Luo, F.L. Meng, K. Qian, Y.T. Wan, J.H. Liu, Porous hierarchical In_2O_3 micro-/nanostructures: preparation, formation mechanism, and their application in gas sensors for noxious volatile organic compound detection, J. Phys. Chem. C 114 (2010) 4887–4894.
[10] C.Y. Lee, S.J. Kim, I.S. Hwang, J.H. Lee, Glucose-mediated hydrothermal synthesis and gas sensing characteristics of WO_3 hollow microspheres, Sens. Actuators B: Chem. 142 (2009) 236–242.
[11] H. Shan, C.B. Liu, L. Liu, J.B. Zhang, H.Y. Li, Z. Liu, X.B. Zhang, X.Q. Bo, X. Chi, Excellent toluene sensing properties of SnO_2—Fe_2O_3 interconnected nanotubes, ACS Appl. Mater. Interfaces 5 (2013) 6376–6380.
[12] N. Yamazoe, G. Sakai, K. Shimanoe, Oxide semiconductor gas sensors, Catal. Surv. Asia 7 (2003) 63–75.
[13] J.H. Lee, Gas sensors using hierarchical and hollow oxide nanostructures: overview, Sens. Actuators B: Chem. 140 (2009) 319–336.
[14] H. Zhang, Q. Zhu, Y. Zhang, Y. Wang, L. Zhao, B. Yu, One-pot synthesis and hierarchical assembly of hollow Cu_2O microspheres with nanocrystals-composed porous multishell and their gas-sensing properties, Adv. Funct. Mater. 17 (2007) 2766–2771.
[15] D.H. Zhang, C. Li, S. Han, X.L. Liu, T. Tang, W. Jin, C.W. Zhou, Electronic transport studies of single-crystalline In_2O_3 nanowires, Appl. Phys. Lett. 82 (2003) 112–114.
[16] P. Nguyen, H.T. Ng, T. Yamada, M.K. Smith, J. Li, J. Han, M. Meyyappan, Direct integration of metal oxide nanowire in vertical field-effect transistor, Nano Lett. 4 (2004) 651–657.
[17] D.W. Kim, I.S. Hwang, S.J. Kwon, H.Y. Kang, K.S. Park, Y.J. Chio, K.J. Chio, J.G. Park, Highly conductive coaxial SnO_2—In_2O_3 heterostructured nanowires for Li ion battery electrodes, Nano Lett. 7 (2007) 3041–3045.
[18] M. Liess, Electric-field-induced migration of chemisorbed gas molecules on a sensitive film – a new chemical sensor, Thin Solid Films 410 (2002) 183–187.
[19] N. Singh, C. Yan, P.S. Lee, Room temperature CO gas sensing using Zn-doped In_2O_3 single nanowire field effect transistors, Sens. Actuators B: Chem 150 (2010) 19–24.
[20] M.W.K. Nomani, D. Kersey, J. James, D. Diwan, T. Vogt, R.A. Webb, G. Koley, Highly sensitive and multidimensional detection of NO_2 using In_2O_3 thin films, Sens. Actuators B: Chem. 160 (2011) 251–259.
[21] M. Epifani, E. Comini, J. Arbiol, E. Pellicer, P. Siciliano, G. Faglia, J.R. Morante, Nanocrystals as very active interfaces: ultrasensitive room-temperature ozone sensors with In_2O_3 nanocrystals prepared by a low-temperature sol–gel process in a coordinating environment, J. Phys. Chem. C 111 (2007) 13967–13971.
[22] P. Li, H.Q. Fan, Y. Cai, M.M. Xu, Zn-doped In_2O_3 hollow spheres: mild solution reaction synthesis and enhanced Cl_2 sensing performance, CrystEngComm 16 (2014) 2715–2722.
[23] D. Han, P. Song, H.H. Zhang, H.H. Yan, Q. Xu, Z.X. Yang, Q. Wang, Flower-like In_2O_3 hierarchical nanostructures: synthesis, characterization, and gas sensing properties, RSC Adv. 4 (2014) 50241–50248.
[24] L. Gao, F.M. Ren, Z.X. Cheng, Y. Zhang, Q. Xiang, J.Q. Xu, Porous corundum-type In_2O_3 nanoflowers: controllable synthesis, enhanced ethanol-sensing properties and response mechanism, CrystEngComm 17 (2015) 3268–3276.
[25] Q. Wan, T.H. Wang, Single-crystalline Sb-doped SnO_2 nanowires: synthesis and gas sensor application, Chem. Commun. 384 (2005) 3841–3843.
[26] T. Zhang, F.B. Gu, D.M. Han, Z.H. Wang, G.S. Guo, Synthesis, characterization and alcohol-sensing properties of rare earth doped In_2O_3 hollow spheres, Sens. Actuators B: Chem. 177 (2013) 1180–1188.
[27] X.H. Liu, J. Zhang, L.W. Wang, T.L. Yang, X.Z. Guo, S.H. Wu, S.R. Wang, 3D hierarchically porous ZnO structures and their functionalization by Au nanoparticles for gas sensors, J. Mater. Chem. 21 (2011) 349–356.
[28] J.W. Yoon, H.J. Kim, I.D. Kim, J.H. Lee, Electronic sensitization of the response to C_2H_5OH of p-type NiO nanofibers by Fe doping, Nanotechnology 24 (2013) 444005.
[29] J. Zhao, T.L. Yang, Y.P. Liu, Z.Y. Wang, X.W. Li, Y.F. Sun, Y. Du, Y.C. Li, G.Y. Lu, Enhancement of NO_2 gas sensing response based on ordered mesoporous Fe-doped In_2O_3, Sens. Actuators B: Chem. 191 (2014) 806–812.
[30] L.P. Gao, Z.X. Cheng, Q. Xiang, Y. Zhang, J.Q. Xu, Porous corundum-type In_2O_3 nanosheets: synthesis and NO_2 sensing properties, Sens. Actuators B: Chem. 208 (2015) 436–443.
[31] Z.X. Cheng, L.Y. Song, X.H. Ren, Q. Zheng, J.Q. Xu, Novel lotus root slice-like self-assembled In_2O_3 microspheres: synthesis and NO_2-sensing properties, Sens. Actuators B: Chem. 176 (2013) 258–263.
[32] P. Li, H.Q. Fan, Y. Cai, M.M. Xu, C.B. Long, M.M. Li, S.H. Lei, X.W. Zou, Phase transformation (cubic to rhombohedral): the effect on the NO_2 sensing performance of Zn-doped flower-like In_2O_3 structures, RSC Adv. 4 (2014) 15161–15170.
[33] Z.F. Liu, T. Yamazaki, Y. Shen, T. Kikuta, N. Nakatani, Influence of annealing on microstructure and NO_2-sensing properties of sputtered WO_3 thin films, Sens. Actuators B: Chem. 128 (2007) 173–178.
[34] A.T. Mane, S.T. Navale, V.B. Patil, Room temperature NO_2 gas sensing properties of DBSA doped PPy—WO_3 hybrid nanocomposite sensor, Org. Electron. 19 (2015) 15–25.
[35] L. Francioso, A. Forleo, S. Capone, M. Epifani, A.M. Taurino, P. Siciliano, Nanostructured In_2O_3—SnO_2 sol–gel thin film as material for NO_2 detection, Sens. Actuators B: Chem. 114 (2006) 646–655.
[36] M. Ivanovskaya, A. Gurlo, P. Bogdanov, Mechanism of O_3 and NO_2 detection and selectivity of In_2O_3 sensors, Sens. Actuators B: Chem. 77 (2001) 264–267.
[37] S. Suarez, J.A. Martin, M. Yates, R. Avila, J. Blanco, N_2O formation in the selective catalytic reduction of NO_x with NH_3 at low temperature on CuO-supported monolithic catalysts, J. Catal. 229 (2005) 227–236.
[38] L. Chen, Z.C. Si, X.D. Wu, D. Weng, DRIFT study of CuO—CeO_2—TiO_2 mixed oxides for NO_x reduction with NH_3 at low temperatures, ACS Appl. Mater. Interfaces 6 (2014) 8134–8145.

Biographies

Xiaolong Hu received his BS degree from the Electronics Science and Engineering Department, Jilin University, China in 2011. Presently, he is a Ph.D. student, majored in microelectronics and solid state electronics. Now, he is engaged in the synthesis and characterization of the semiconducting functional materials and gas sensors.

Liyuan Tian received the BE degree in Department of Electronic Science and Engineering in 2014. She is currently studying for her MS degree in College of Electronic Science and Engineering, Jilin University, China.

Hongbin Sun received the BE degree in Department of Electronic Science and Engineering in 2014. He is currently studying for his MS degree in College of Electronic Science and Engineering, Jilin University, China.

Biao Wang obtained his Ph.D. degree from Jilin University, China in 2008. Now he is an associate research professor in Changchun Institute of Optics, Fine Mechanics and Physics, Chinese Academy of Science. His current research is laser gas sensor.

Yuan Gao received her Doctor's degree in Department of Analytical Chemistry at Jilin University in 2012. Now she is a lecturer in Jilin University, China. Her current research is focus on the preparation and application of graphene oxide and semiconductor oxide, especial in gas sensor and biosensor.

Peng Sun received his Ph.D. degree from the Electronics Science and Engineering department, Jilin University, China in 2014. Now, he is engaged in the synthesis and characterization of the semiconducting functional materials and gas sensors.

Fengmin Liu received the BE degree in Department of Electronic Science and Technology in 2000. She received his Doctor's degree in College of Electronic Science and Engineering at Jilin University in 2005. Now she is a professor in Jilin University, China. Her current research is preparation and application of semiconductor oxide, especial in gas sensor and solar cell.

Geyu Lu received the BS degree in electronic sciences in 1985 and the MS degree in 1988 from Jilin University in China and the Dr. Eng. degree in 1998 from Kyushu University in Japan. Now he is a professor of Jilin University, China. Presently, he is interested in the development of functional materials and chemical sensors.